https://dx.doi.org/10.22161/ijaers.77.15 ISSN: 2349-6495(P) | 2456-1908(O)

Multi-function Hybrid Microgrid with Four-Leg Voltage Source Inverter

José Francisco Resende da Silva[1], John Freddy Franco Baquero[1], Fabio de Oliveira Ferreira[2], Hugo Villela de Miranda[2], Thobias Antônio Cândido Pereira[2], Marcos Paulo Gonçalves Rodrigues[2], Rafael Nielson[3]

[1]Department of Energy Engineering, São Paulo State University - UNESP, Rosana-SP, Brazil
[2]Department of Research TracelLtda, Duque de Caxias-RJ, Brazil
[3]Research and Development Enel Distribution Goiás, Goiania -GO, Brazil

Abstract*—*Unintentional islanding of distributed generation systems is generally avoided as a safety measure implied by worldwide electrical standards. Considering current grid technologies with better sensing capabilities and semiconductor devices with novel capabilities that allow faster response times and higher maximum ratings, there are some applications where distributed resources could improve reliability in the case of intentional islanding. Safe microgrid equipment with better isolation and control features allows efficient use of energy surplus whenever grid fault events occur, feeding emergency energy to critical loads. In this context, a 20 kW hybrid on-grid/off-grid multi-function microgridis presented along with a simplified approach for designing the contained power inverter used with intentional islanding function.

Keywords*—*Distributed generation, hybrid inverter, microgrid equipment.

I. INTRODUCTION

The market of distributed generation (DG) in Brazil is in constant growth, reaching sales of 1.07 billion dollars in 2018, with turnover exceeds up to 978 MWp (megawatt peak), according to a study published by Greener Brasil (based on data from Federal Revenue Service, Greener Brasil, and ANEEL) [1], where growth continues at extremely high rates, despite Brazil's economic and political situation. In 2017 there were approximately 21,998 DG connections and in December of 2018, they totaled 52,852 (a growth rate of 140%), with a variation from 184.8 MWp installed capacity to 545.6 MWpbetween 2017 to 2018, respectively. Substantial growth is occurring even in a period of recessive economy, with the evolution of micro and macro economic reforms in progress, especially what will ensue the recent approval of the Brazilian pension reform bill. A positive impact is expected for maintaining the incentives for generation systems because their market is small compared to other developed countries. Estimates point more than 80 million consumer sites where it would be viable to have energy production reconciled with consumption, therefore there is still a gigantic potential for growth of the accumulated DG market (MWp).

A developed microgrid system meets five aspects solved by market only through distinct equipment: 1) solar inverters operating with nominal power of 20 kW, that can be cascaded in modules with total power up to 2MW; 2) uninterruptible power supplies (UPS); 3) local and remote power flow management; 4) auxiliary power unit integration, such as battery banks and fuel cells, to extend reserve power; 5) automatic transfer switch systems for utility grid interconnection. Developed technology consist in a set of control boards: central microprocessor control module, gate drive, sensor data module, communication interface, and human-machine interface. This device is suitable for integrating distributed generation of solar energy networks as a local source, providing greater energy efficiency and, consequently, accelerated investment gains, whose development initially targets theoretical studies to integrate DC photovoltaic generation and battery storage systems. Fig. 1 presents the hybrid microgrid topology to feed critical loads through a solar energy source and battery.

https://dx.doi.org/10.22161/ijaers.77.15 *ISSN: 2349-6495(P) | 2456-1908(O)*

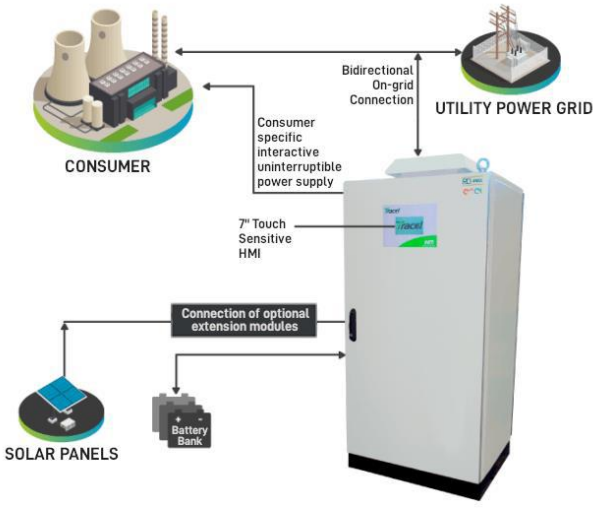

Fig.1: Presented hybrid multi-function microgrid.

A main component of the system is the four-leg voltage source inverter. Two types of power inverters are generally available in market when considering main grid connection or isolation: off-grid and on-grid inverters. Off-grid inverters are intended to provide energy from DC-generated sources such as photovoltaic power to isolated consumers in alternating current, referred to as island mode operation. On the other hand, on-grid inverters use energy from DC sources to feed alternating current as well as to inject, if possible, surplus energy to the main grid. Although not yet officially available in the Brazilian market, on-grid inverters with off-grid function allow both modes of operation, connected or isolated from the main grid. Unintentional islanding of distributed generation systems is generally avoided as a safety measure implied by worldwide electrical standards. Considering current grid technologies with better sensing capabilities and semiconductor devices with novel capabilities that allow faster response times and higher maximum ratings, there are some applications where distributed resources could improve reliability in the case of intentional islanding. In this paper, we propose a simplified methodology to develop power inverters and a working prototype four-leg voltage source inverter used with the hybrid microgrid system that ensures safe isolation and power to critical loads during grid fault events. The remaining of this paper is organized as follows: Section II presents the power inverter market in Brazil and functionality, Section III the considered power inverter design approach, Section IV case study of the microgrid system, simulations and obtained results for the 20 kW prototype.

II. POWER INVERTER MARKET AND FUNCTIONALITY

An important share of the renewable sources applied in distributed generation market, solar energy in Brazil has great prospects. According to the US Department of Energy, Brazil has a significant potential for renewable energy generation, where in 2024 is estimated at 7GWp of installed capacity. With current legislation and regulations, the investment forecast for the year 2030 is $21 billion. There may be a variation in growth of this market with the revision of Resolution 482/2012 of ANEEL, currently underway, which is expected to introduce a form of compensation to the electric distribution companies from using the grid to compensate energy generation and consumption. This change probably will reduce investment returns on systems as of 2020.

Current business models must comply with standards as well as design, manufacturing and installation restrictions of system components, where modular configurations are more capable of adapting to different applications. Among existing equipment configurations, the DC power supply type may vary considering the ability to integrate photovoltaic generator units, wind generators, hydrogen fuel cells, biofuel motor-generator sets. Other equipment include battery banks, DC/DC converters, Uninterruptible Power Supply (UPS) controllers, and rectifiers depending on load type and expected power availability.

In Brazil, UPS is commonly referred as no-break, and attend a significant portion of the commercial, industrial and residential sectors, such as apartment complexes and rural businesses. Today, according to [3], this market is estimated at $400 million, with production of large equipment (from 3 to 500 kVA) around 100,000 units/year. An important feature of a UPS is the time to reestablish energy, which should be less than one period of the sine waveform – given the standard 60 Hz grid frequency would correspond to approximately 15ms. There are recent products in the market promoted as short-breaks, which, for less demanding applications, energy is reestablished in a longer period, usually two or three periods (30-45ms), maybe providing an ideal cost-benefit for systems that can support brief discontinuities.

The presented inverter topology consists of a bridge configuration, whose main advantage according to [4] is to lessen wear of commutating components, such as from current spikes, overvoltage and over temperature. Fig. 1 is the basic arrangement used for the hybrid inverter considered for the project, denominated as the Three-phase Four Leg Voltage Source Inverter (FLVSI). Circuit input is a DC voltage source with a cap filter, followed by

https://dx.doi.org/10.22161/ijaers.77.15 *ISSN: 2349-6495(P) | 2456-1908(O)*

switching components and output stage with caps that correspond to each phase. Switching components consist in Isolated Gate Bipolar Transistors (IGBTs), which allow high frequency modulation, available in market with efficiency and life cycle characteristics that present good performance for power converter equipment.

One of the main challenges in DC/AC converter design is minimizing switching losses and parasitic circuit elements, which prevent efficient operation in high power applications. The so-called "dead times" during switching cycles can be seen as short-circuits to the source caused by premature state changes, which should be avoided. Another point to have in mind is that inverter operation should suffer little influence from the applied load, where the extreme conditions would be damage to the components when there is no load present (open circuit) and when load low impedance (short circuit).

There are several techniques used to generate high-frequency switching, the simplest known as Pulse Width Modulation (PWM). There are several PWM techniques, among them the most implemented [6] is the sine wave PWM, or SPWM, due to its relative simplicity. The modulating signal to control gate triggering is from the comparison of a sine wave (Vcontrol) with a triangular carrier wave (Vtri), illustrated by Fig. 2. Upper gate devices are turned on releasing current when polarization voltage is positive and blocked when voltage is negative. Lower gate devices have a similar scheme to conduct negative voltage when upper gates are blocked.

When the output phases are not balanced, even though the angular difference is 120°, there is an undesirable common mode voltage fed to consumers that can damage equipment. To reduce common mode voltage, [7-11] suggest that the neutral connection obtained from the inverter topology be controlled from a fourth leg parallel to the switching bridge, providing a means to adjust the neutral voltage point so that it is symmetrical with respect to the phases.

III. POWER INVERTER DESIGN APPROACH

When designing a new inverter, this primarily involves determining switching element specifications and the thermal dissipation layout. After defining the inverter topology type, the next step is to solve (1)–(12) to obtain an estimate of IGBT characteristics, to select a semiconductor for this design, and (13)–(21) to obtain a suitable heatsink. Among other variables, the DC source characteristics, expected input voltage, and voltage and power requirements at output are needed to begin.

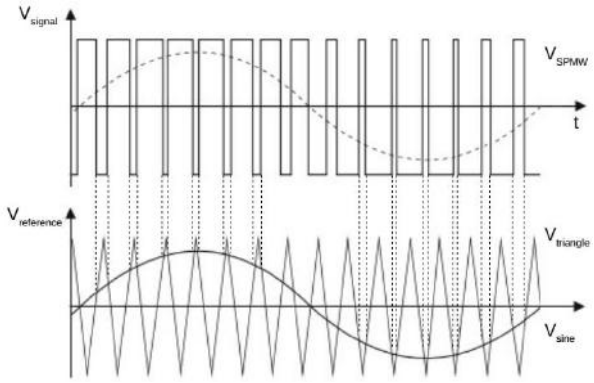

Fig: 2: Control signal obtained from sine wave reference and triangular carrier wave.

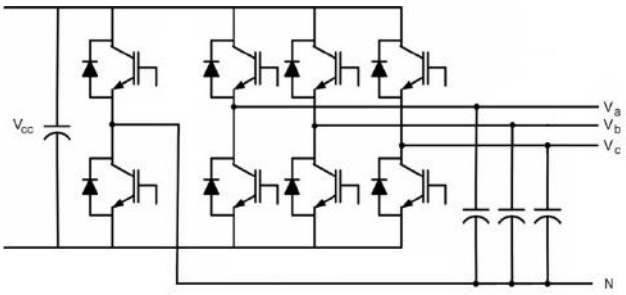

Fig. 3: Basic full bridge switching topology.

A. Determining Switching Element Specifications

The amplitude modulation index (ma) can be expressed by the ratio of theoretical output peak-to-peak voltage and the input voltage:

$$m_a = \frac{\sqrt{2}\cdot V_{ORMS}}{\sqrt{3}} \frac{2}{Vi_{min}} \quad (1)$$

where V_{ORMS} is the nominal AC output voltage and Vimin is the minimum DC input voltage. The inverter must supply output the specified voltage when the input voltage is at its lowest, this constraint is not a problem when the input voltage is higher.

The modulation index should not exceed 1.0, in this case there is over modulation which means that with the SPWM technique the amplitude of the first harmonic is not linearly proportional to the modulation index [11]. There are improvements such as third-harmonic injection (THI-SPWM) where the idea is to add a third harmonic of the reference sine wave to flatten the region of peak voltage, increasing linear range of operation. Because third harmonic components are equally applied to the three phases this would not compromise output phase generated by the inverter. Since the objective was to present a simple

https://dx.doi.org/10.22161/ijaers.77.15 *ISSN: 2349-6495(P) | 2456-1908(O)*

methodology of inverter design, the details regarding these techniques is out of scope of this paper.

The output voltage wave form with SPWM modulation for a given phase is expressed by:

$$V_{Opeak} = m_a \cdot \frac{V_i}{2} \cdot \sin(\omega t + \varphi) \quad (2)$$

where φ is the waveform phase and V_i the DC input voltage. The theoretical apparent power (P_{AP}) is estimated from:

$$P_{AP} = \frac{P_{AT}}{\cos\theta} \quad (3)$$

where P_{AT} is the expected active power and $\cos\theta$ is the expected power factor. The nominal current is expressed by the equation:

$$I_{O\,RMS} = \frac{Pot_{AP}}{\sqrt{3} \cdot V_{O\,RMS}} \quad (4)$$

Output equivalent load and inductance is, respectively:

$$Req = \frac{Pot_{AP}}{(\sqrt{3} \cdot I_{O\,RMS})^2} \quad (5)$$

$$Leq = \frac{\sqrt{P_{AP}^2 - P_{AT}^2}}{(\sqrt{3} \cdot I_{O\,RMS})^2} \cdot \frac{1}{(2\pi \cdot F_O)} \quad (6)$$

The current applied to the IGBT module is equivalent to output peak current, thus:

$$Ip_{IGBT} = I_{ORMS} \cdot \sqrt{2} \quad (7)$$

Freewheeling diodes in parallel to the IGBTs at peak power dissipate approximately the same peak output current:

$$I_{peak\,diode} = I_{O\,peak} \quad (8)$$

Nominal and average current integrations for the IGBT modules considering SPWM switching [12] are:

$$I_{RMS} = \frac{\sqrt{2}}{2} \cdot \sqrt{\frac{1}{\pi}\left(\frac{1}{4} \cdot I_{O\,peak}^2 \cdot \pi + \frac{2}{3} \cdot I_{O\,peak}^2 \cdot m_a \cdot \cos\theta\right)} \quad (9)$$

$$I_m = \frac{1}{2\pi}\left(I_{O\,peak} + \frac{1}{4} I_{O\,peak} \cdot m_a \cdot \cos\theta\,\pi\right) \quad (10)$$

Nominal and average current integrations for the freewheeling diodes considering SPWM switching [12] are:

$$I_{RMS\,diode} = \frac{\sqrt{2}}{2} \cdot \sqrt{\frac{1}{\pi}\left(\frac{1}{4} \cdot I_{O\,peak}^2 \cdot \pi - \frac{2}{3} \cdot I_{O\,peak}^2 \cdot m_a \cdot \cos\theta\right)} \quad (11)$$

$$I_{mdiode} = \frac{1}{2\pi}\left(I_{O\,peak} - \frac{1}{4} I_{O\,peak} \cdot m_a \cdot \cos\theta\,\pi\right) \quad (12)$$

B. Thermal Dissipation Layout

The cooling of the device occurs through forced air conduction through heatsinks in contact with the active elements. The next equations followed the schematic shown in Fig. 4, where *Rth-jc* is the thermal resistance of each component to its packaging; *Rth-cs* – thermal resistance of the packaging; *Rth-ds* – thermal resistance of the heatsink; *Tj* – junction temperature; *Pigbt* – power dissipated by the IGBT; *Pdiode* – power dissipated by the freewheeling diode; *Pmod* – power dissipated by the IGBT-diode pair module.

The sum of the power dissipation occurring in conduction and switching in each IGBT is described by (13-14), considering the adjustment of the parameters Eon and Eoff, the dissipated energies for switch turn on or off, respectively, corrected for the chosen operating voltage and current.

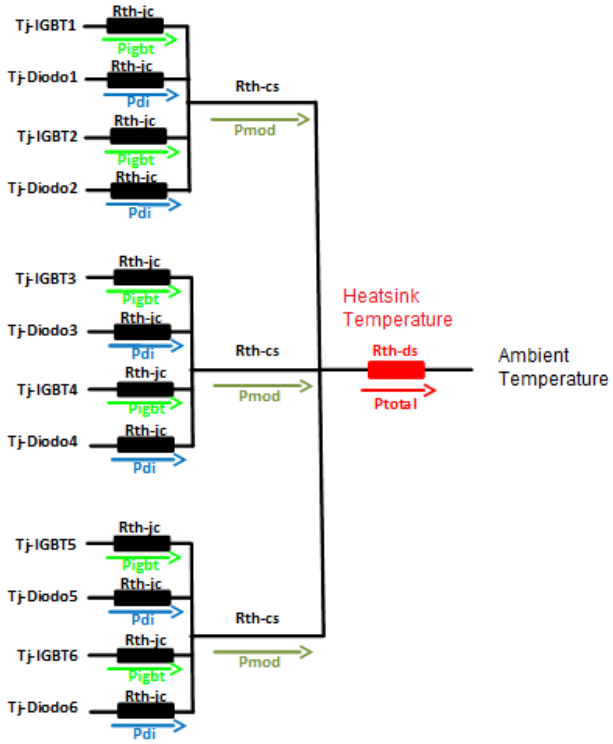

Fig. 4: Thermal schematic to determine heatsink characteristics.

$$P_{IGBT} = V_{CEO} \cdot Im_{IGBT} + R_{ce} \cdot Irms_{IGBT}^2 + P_{E\,IGBT} \quad (13)$$

$$P_{EIGBT} = Fch \cdot (E_{on} + E_{off}) \cdot \left(\frac{V_{in}}{V_{IGBTmax}}\right)^{Kv} \cdot \left(\frac{Ip_{IGBT}}{I_{IGBTmax}} \cdot \frac{\sqrt{2}}{\pi}\right)^{Ki} \quad (14)$$

https://dx.doi.org/10.22161/ijaers.77.15 *ISSN: 2349-6495(P) | 2456-1908(O)*

whereV_{CEO} is the colector-emitter voltage and R_{ce} is the collector-emitter impedance of each IGBT obtained from the manufacturer datasheet. K_V and K_I are constants equal to 1.4 and 1.0, respectively.

The power dissipated from each freewheeling diode, considering the influence of the parameter E_{rec}, reverse energy recover, for operating voltage and current conditions:

$$P_{diode} = V_{to} \cdot Im_{diode} + R_t \cdot Irms^2_{diode} + P_{E\,diode} \quad (15)$$

$$P_{Ediode} = E_{rec} \cdot \left(\frac{V_{in}}{V_{diodemax}}\right)^{K_V} \cdot \left(\frac{Ip_{diode}}{I_{diodemax}} \cdot \frac{\sqrt{2}}{\pi}\right)^{K_I} \quad (16)$$

whereV_{to} and R_t are the voltage and impedance of forward polarization of the diode obtained form the datasheet specifications.

The module type chosen is a pair of IGBTs and diodes. The dissipated power by a single module is:

$$P_{mod} = 2 \cdot (P_{IGBT} + P_{diode}) \quad (17)$$

The total dissipation in a switching cycle is given by:

$$P_{total} = 3 \cdot P_{mod} \quad (18)$$

The junction temperature can be estimated as 85% of the maximum junction temperature especified for the IGBT, as a reasonable margin. The thermal resistance of the heatsink (Rthdiss) is in function of a chosen ambient temperature (T_{AMB}):

$$Rth_{diss} = \frac{Tj_{IGBTmax} - (T_{AMB} + P_{IGBT} \cdot Rth_{IGBT} + P_{mod} \cdot Rth_{mod})}{Ptotal} \quad (19)$$

We can calculate the junction temperature of the IGBT with the obtained with the heatsink's thermal resistance:

$$Tj_{IGBT} = T_{AMB} + Rth_{diss} \cdot P_{total} + P_{mod} \cdot Rth_{IGBT} + P_{IGBT} \cdot Rth_{\text{mod-IGBT}} \quad (20)$$

The heatsink'stemperature estimate is expressed by:

$$T_{diss} = T_{AMB} + Rth_{diss} \cdot P_{total} \quad (21)$$

With the determined thermal resistance and temperature, a sufficient heatsink model can be chosen. An additional module to increase cooling may be required according to the application, whether it be forced ventilation or liquid cooling, to protect components from overheating.

IV. CASE STUDY OF THE HYBRID MICROGRID SYSTEM

Simulations were performed with the PSIM™ software Version 9.1.1.400 where the detailed schematic can be seen in Fig. 5 and 6. Input power is a set of photovoltaic panels with sum of nominal power above 20 kW. The parameters used for the load cell block available in the software took into consideration solar farm plans of 3 rows with 17 panels in series each:

- Open Circuit Voltage: 647,7 Vdc (38,1 Vdc per panel);
- Short Circuit Current: 54.9 A (18,3 A per row);
- Maximum Power Voltage: 521,9 Vdc (30,7 Vdc per panel);
- Maximum Power Current: 51 A (17 A per row).

No specific IGBT model parameters were used, and only cable resistance and inductance were considered. Power dissipated by output filter capacitors are concentrated in series resistors. The MPPT (Maximum Power Point Tracking) strategy programmed into the control block consisted in the Incremental Conductance technique. Resulting simulation waveforms can be seen in Figs. 7 and 8.

Figures 10-13 present data obtained from the Fluke Series II 434 Analyzer, output phase and neutral voltages, output currents, voltage and current harmonic distortion. An image of the 20 kW prototype is presented in Fig. 13.

The inverter's intention is to withstand tests defined by the Conformity Assessment Regulations described in the INMETRO Ordinance No. 357/2014 [13], related to the Conformity Assessment Program for Photovoltaic Energy Systems and Equipment. in addition to the standards ABNT NBR 16149:/2013, ABNT NBR 16150/2013 and ABNT NBR IEC 62116/2012.

According to [13], for equipment conformance labeling, the Conformity Assessment Requirements apply to the following equipment: Photovoltaic modules; Battery Charge/discharge Controllers; inverters for autonomous systems with nominal power between 5 and 10 kW; inverters for systems connected to the grid with rated power up to 10 kW; Battery bank systems. The following procedures for the tests are based on the minimum requirements of the equipment according to current standards:

1. Flickering;
2. DC component injection;
3. Harmonics and waveform distortion;
4. Power factor;
5. Reactive power injection/demand;
6. Over/under voltage;
7. Over/ under frequency;

https://dx.doi.org/10.22161/ijaers.77.15 *ISSN: 2349-6495(P) | 2456-1908(O)*

8. Control of the active power in over frequency;

9. Reconnection;

10. Out-of-phase automatic reclosing;

11. Active power modulation;

12. Reactive power modulation;

13. Disconnection of the photovoltaic system from the grid;

14. Requirements for back-up due to faults in the network;

15. Protection against reversal of polarity;

16. Overload;

17. Anti-islanding. Items 1 through 14 are further defined in standards ABNT NBR 16149/2013 and ABNT NBR 16150/2013, items 15 and 16 are uniquely specified in the same ordinance and item 17 is described in the standard ABNT NBR IEC 62116/2012.

Although there is no precise specification of the standards for hybrid generation and storage systems equipped with static transfer switches, the different test procedures were carried out to ensure the safety and quality of the equipment. Test results for the three-phase four-leg voltage source inverter demonstrated stable operation of the equipment as specified as designed.

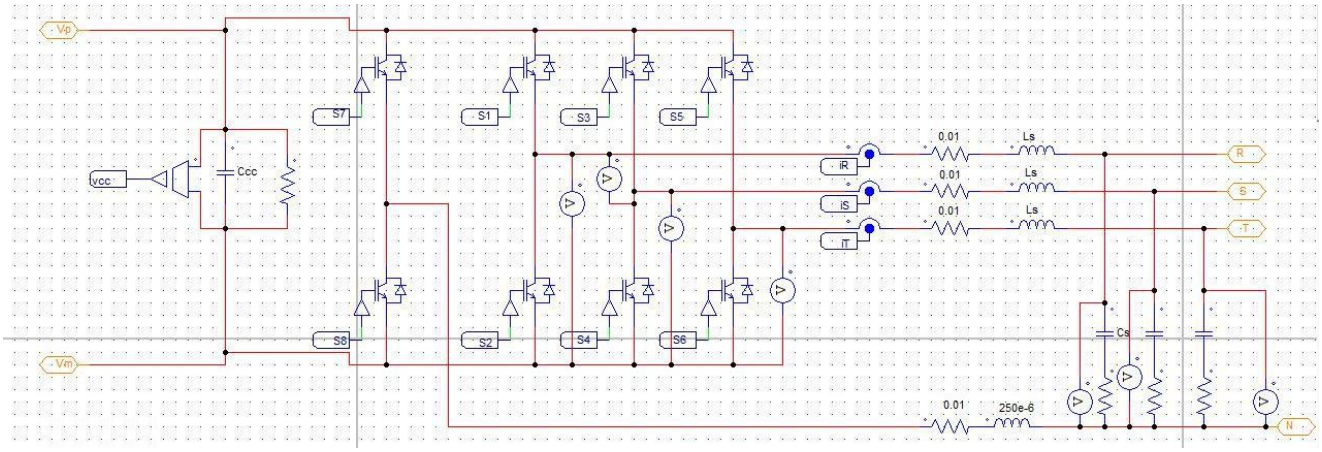

Fig. 5: Hybrid Inverter topology simulation schematic.

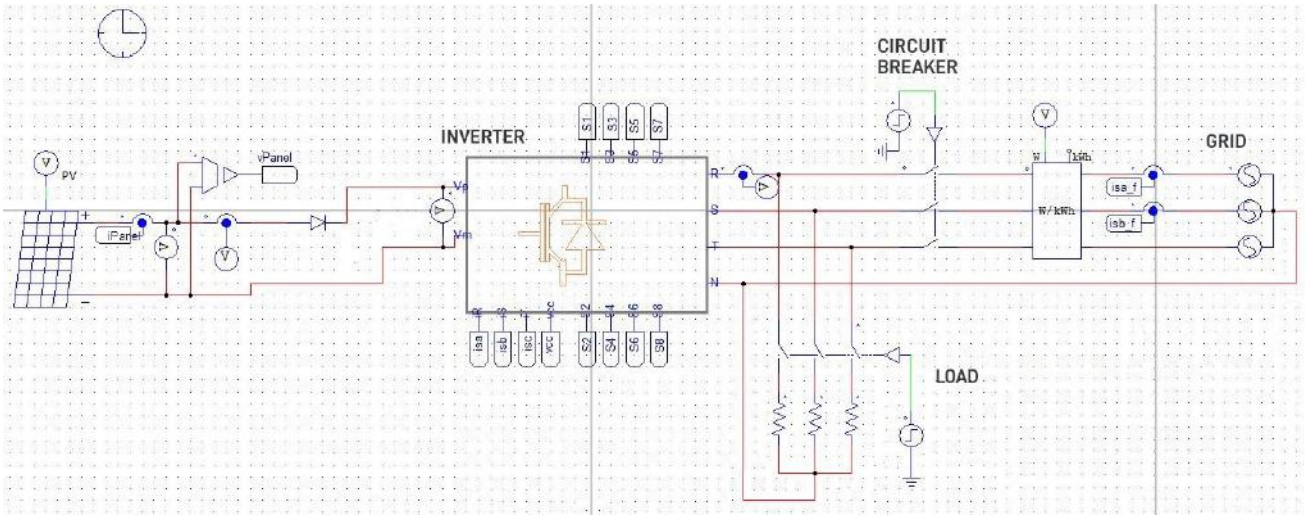

Fig. 6: FLVSI inverter simulation submodule schematic.

https://dx.doi.org/10.22161/ijaers.77.15 *ISSN: 2349-6495(P) | 2456-1908(O)*

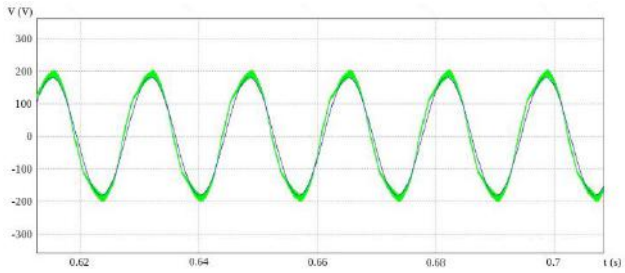

Fig. 7: Simulated single phasevoltage and current output.

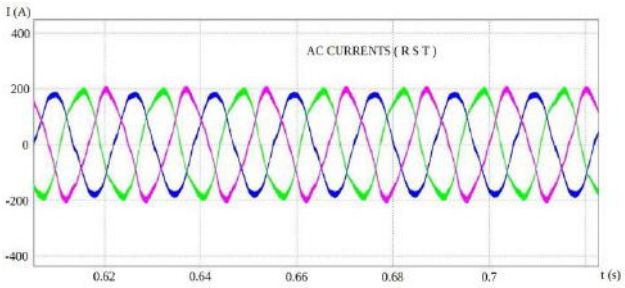

Fig. 8: Simulated output three-phase current.

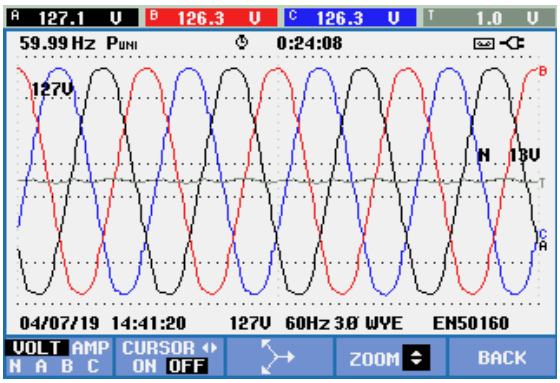

Fig. 9: Prototype output phase and neutral voltages.

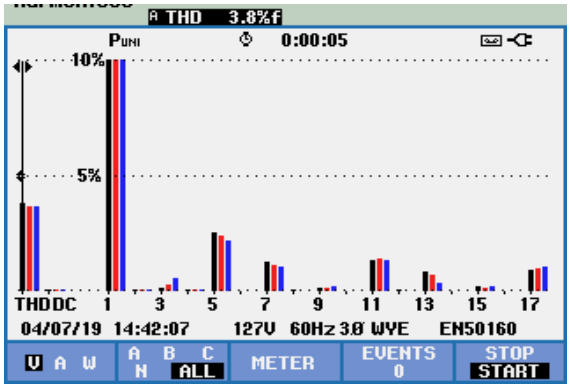

Fig. 10: Voltage Harmonic Distortion.

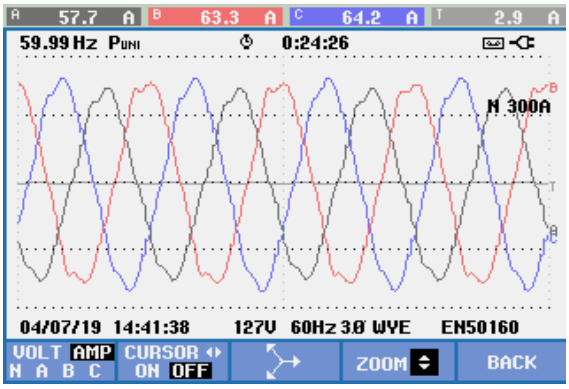

Fig. 11: Prototype output currents.

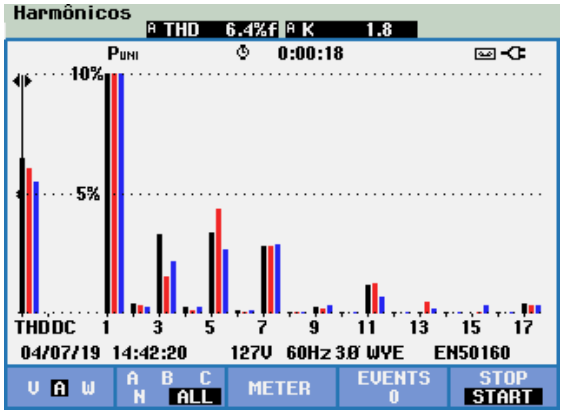

Fig. 12: Current Harmonic Distortion.

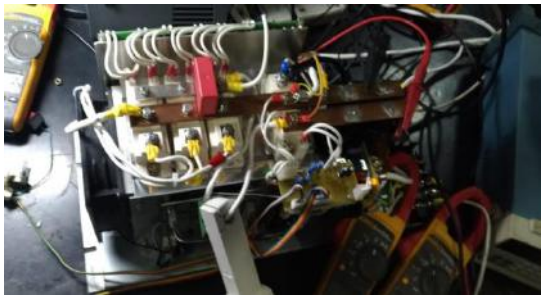

Fig. 13: Experimental setup of the FLVSI Inverter.

V. CONCLUSIONS

We thereby present a simple design methodology for power inverters and a working prototype with perspective to contribute to the development of Brazilian regulations regarding solar inverters above 10 kW and hybrid on-grid/off-grid systems.

In order to certify distributed generation equipment, it is necessary to submit them to the tests specified by [13], not designed specifically for hybrid inverters. Regulations also do not require certification of inverters above 10 kW.

https://dx.doi.org/10.22161/ijaers.77.15 *ISSN: 2349-6495(P) | 2456-1908(O)*

We hope that our development will contribute to develop certification processes in Brazil regarding applied technologies.

ACKNOWLEDGEMENTS

This research was sponsored by the Brazilian Agency of Electical Energy (ANEEL), Enel Group Goiás, and Tracel Ltda. Important contributions to this work were made from the technical staff of Tracel and U. A. Miranda.

REFERENCES

[1] Strategic Market Study: Photovoltaic Sector - Distributed Generation, 3rd Quarter of 2019. www.greener.com.br, Oct. 2019.
[2] "IEEE Guide for Design, Operation, and Integration of Distributed Resource Island Systems with Electric Power Systems," Jul. 2011.
[3] In Portuguese: RevistaPotência, "Elétrica, Iluminação, Automação, Sustentabilidade e SistemasPrediais. Estrutura laboratorial," ed. 119, Nov. 2015.
[4] N. Mohan, T. M. Undeland, and W. P. Robbins, Power Electronics Converters Applications and Design. 3rd ed. John Wiley & Sons Inc, 2003.
[5] R. Teodorecsu, M. Liserre, and P. Rodríguez, Grid Converterss for Photovoltaic and Wind Power Systems, John Wiley & Sons Inc, 2011.
[6] N. L. Raghuram and J. H. Suresh, "A Critical Study of Modulation Techniques for Three Level Diode Clamped Voltage Source Inverter for Grid Connection of WECS," 1st International Conference on Electrical Energy Systems (ICEES), pp. 221-226, 2011.
[7] J. Huang, R. Xiong, Z. Wang, W. Zuo, Y. Zhou, H. Shi, "A Novel SPWM Control Strategy to Reduce Common-Mode Voltage in Three Phase Four-Leg Inverters," International Conference on Electrical Machines and Systems (ICEMS), pp. 1526-1530, 2008.
[8] J. Bastidas-Rodríguez and C. Ramos-Paja, "Types of inverters and topologies for microgrid applications," UIS Ingenierías, vol. 16, no. 1, pp. 7-14, Dec. 2016.
[9] A. L. Julian, T. A. Lipo, and G. Oriti, "Elimination of Common-Mode Voltage in Three Phase Sinusoidal Power Converters," PESC Record. 27th Annual IEEE Power Electronics Specialists Conference, pp. 1968-1972, Jun. 1996.
[10] T. Hornik and Q. Zhong, "H∞ current control strategy for the neutral point of a three-phase inverter," 2011 50th IEEE Conference on Decision and Control and European Control Conference (CDC-ECC), December, 2011.
[11] In Portuguese: R. M. Stephan, Acionamento Comando e Controle de Máquinas Elétricas, Ciência Moderna, 2013.
[12] A. K. Sadigh, V. Dargahi, and K. A. Corzine, "Investigation of conduction and switching power losses in modified stacked multicell converters", IEEE Transactions on Industrial Electronics, Vol. 63, No. 12, Dec. 2016.
[13] In Portuguese: INMETRO Ordinance No. 357/2014, "PortariaInmetro nº357, de 01 de agosto de 2014," www.inmetro.gov.br, Aug. 2014.